



# Using the Reflection Ellipsometry to Detect the Stress for the Gold Coating Reflection Mirrors

Chenyu Wang<sup>1,2</sup> · Wei Liu<sup>3</sup> · Yu Niu<sup>3</sup> · Wei Sha<sup>4</sup> · Ziren Luo<sup>3</sup>

Received: 2 March 2022 / Accepted: 15 September 2022 / Published online: 26 September 2022  
© The Author(s), under exclusive licence to Springer Nature B.V. 2022

## Abstract

The residual stress information of the precision surface optical device with a metal coating plays an important role in precision optical manufacturing. However, the conventional optical-based non-contact approaches fail to measure the stress less than MPa for such devices, which is required for high precision gravitational waves detection. To solve this problem, we use ellipsometry to detect the stress of a gold coating reflection mirrors as the first trial. Under the pseudo-Brewster angle of the gold, the stress sensitivity for the ellipsometry amplitude  $\psi$  reaches 35 kPa. The results suggest the traditional reflection ellipsometry responses at two specific orthogonal directions can be used to measure the strain-induced dielectric function tensor variations under a uniaxial stress situation. A preliminary microscopic model based on Drude model is proposed to derive the relationship between the dielectric function tensor variation of the coating and the uniaxial tensile strain  $s$ . Thus, the reflection ellipsometry can be used as an alternative method for the residual stress detection for the high precision planar optical devices with metal coatings under a uniaxial stress condition.

**Keywords** Stress · Metal coating · Ellipsometry · High precision

## Introduction

The gravitational waves (GWs) detection has become a hot topic since the successful discovery of GWs by the LIGO collaboration in 2015, and the space-based GWs detection

has emerged as the next exciting goal for the future gravitational universe research for the space-based GWs detection would be able to detect a larger spectrum of the gravitational radiation sources than the ground-based GWs detection (Abbott et al. 2016a, b, 2017; Dubert et al. 2019; Brown et al. 2021). The Taiji program, one of the space-based GWs detection scheme, is designed to detect GWs with frequencies ranging from 0.1 mHz to 1.0 Hz, with a sensitivity of  $1 \text{ pm}/\sqrt{\text{Hz}}$  (Hu and Wu 2017; Liu et al. 2018; Luo et al. 2021). Various important technologies must be rigorously verified in order to reach such a high range of accuracy, especially the telescope system and the stability of the optical platform in the satellite both of which greatly affect the ranging precision (Luo et al. 2020). To ensure that the scientific goals are achieved smoothly, it is necessary to detect and evaluate the stress of the precision optical coating devices such as the telescopes under the aerospace loads (Shen et al. 2022), and the residual stress which has considerable practical value and governs the device design and the subsequent processing. Therefore, how to obtain the residual stress information of the surface optical coating device accurately and more precisely has become an urgent problem to be solved.

---

This article belongs to the Topical Collection: Research Pioneer and Leader of Microgravity Science in China: Dedicated to the 85th Birthday of Academician Wen-Rui Hu  
Guest Editors: Jian-Fu Zhao, Kai Li

---

Chenyu Wang and Wei Liu contributed equally to this work.

---

✉ Yu Niu  
niuyu@imech.ac.cn

- <sup>1</sup> NML, Beijing Key Laboratory of Engineered Construction and Mechanobiology, Institute of Mechanics, Chinese Academy of Sciences, Beijing 100190, China
- <sup>2</sup> School of Engineering Science, University of Chinese Academy of Science, Beijing 100049, China
- <sup>3</sup> Center for Gravitational Wave Experiment, Institute of Mechanics, Chinese Academy of Science, Beijing 100190, China
- <sup>4</sup> State Key Laboratory of Applied Optics, Fine Mechanics and Physics (CIOMP), Changchun Institute of Optics, Chinese Academy of Sciences, Changchun 130033, China

The traditional residual stress measurement schemes consist of contact schemes and non-contact ones. Current typical contact measurement schemes, mainly including mechanical and electrical sensors such as piezoelectric acceleration sensors, piezoelectric films, and resistance strain gauges, are limited by the need for non-destructive surface measurement with high precision, wide frequency range, and simple installation (Roos et al. 1996). For example, contact schemes are not appropriate to the test of optical devices with high-precision requirements such as telescopes. Therefore, the optical-based non-contact approach has become the preferred choice to achieve the goal, including X-ray diffraction (Labat et al. 2000), Stoney curvature (Janssen et al. 2009; Pureza et al. 2009), and micro-Raman spectroscopy (Nakashima et al. 2006; Groth et al. 2016; Li et al. 2017). These approaches are widely used for the metallic glass surface stress measurement with the accuracy of tens of MPa to GPa (Zhang et al. 2006). A second approach is the method based on the stress-induced birefringence of the transparent materials, such as digital photoelastic (Ramesh and Ramakrishnan 2016), photoelastic modulator, and polarized cavity ring-down spectroscopy (van der Sneppen et al. 2006). Although the stress accuracy of the second approach has been further improved to kPa (Guo et al. 2018; Xiao et al. 2018), the scheme can hardly be applied to the metal film coating device because of the absorption of the metal. As a result, a stress detection method for the metal film coating device is needed with a high accuracy, better than MPa. Therefore, how to obtain the residual stress information of the surface optical device with a metal coating accurately has become an urgent problem to be solved.

As a phase-sensitive optical technique, ellipsometry is traditionally used to measure the changes of optical properties of thin films effectively. Due to its high sensitivity, fast measurement speed, and undamaged nature of examination, it has been fully concerned with and applied in the biological (Sun and Zhu 2014; Jin and Niu 2017; Niu and Jin 2017) and semiconductor industry (Pflitsch et al. 2006; Gu et al. 2019). As a consequence, this paper proposes to develop a set of stress sensing technology for a gold film coated device based on the ellipsometric measurement system and the stress on the sample surface's optical characteristics is elucidated under the basic stress condition.

## Ellipsometry for a Uniaxial Compressed Film

The reflection ellipsometry measures the polarization state of the reflections from the interactions between a planar sample surface and the incident light. Since the thickness and the dielectric functions of the interfaces exert a great influence on the light the electric field of which is parallel

to the plane of incidence (p-polarized light) while give little influence on the light the electric field of which is perpendicular to the incident plane (s-polarized light), we take the s-polarized light as the reference to measure the polarization state of the p-polarized light. For an isotropic film, the ellipsometric parameter  $\rho$  can be obtained from a diagonal Jones Matrix  $J = \begin{pmatrix} R_{pp} & 0 \\ 0 & R_{ss} \end{pmatrix}$

$$\rho = \frac{R_{pp}}{R_{ss}} = \tan\psi e^{j\Delta} \quad (1)$$

where  $R_{pp}$  and  $R_{ss}$  are the complex reflection coefficients of p-polarized light and s-polarized light,  $\psi$  is the ellipsometry amplitude and  $\Delta$  the ellipsometry phase.

For an anisotropic interface, the p-polarized light and s-polarized light are related. Thus, the Jones matrix is not diagonal in general, which gives  $J = \begin{pmatrix} R_{pp} & R_{sp} \\ R_{ps} & R_{ss} \end{pmatrix}$  and two more ellipsometric parameters  $R_{sp}$  and  $R_{ps}$  are defined by

$$\begin{aligned} \rho_{sp} &= \frac{R_{sp}}{R_{ss}} = \tan\psi_{sp} e^{j\Delta_{sp}} \\ \rho_{ps} &= \frac{R_{ps}}{R_{pp}} = \tan\psi_{ps} e^{j\Delta_{ps}} \end{aligned} \quad (2)$$

The traditional reflection-based ellipsometry fails because it cannot measure all the ellipsometric parameters to obtain the information of the anisotropic medium. However, for the cases where p-polarized light and s-polarized light can be reflected independently, which gives  $R_{sp} = R_{ps} = 0$ , the conventional ellipsometric parameter  $\rho$  can be used to deduce the sample interface information (Azzam and Bashara 1977).

For a uniaxial compressed film, the optic axis is parallel to the compression direction according to the geometric symmetry. Thus, two cases are considered: the optic axis is parallel to the y-direction which is normal to the plane of incidence. and the optic axis parallel to the x-direction which lies in the plane of the incidence.

On the one hand, for the optic axis parallel to the y-direction, the electric field of the s-polarized light is parallel to the optic axis and converts fully to the extraordinary mode (with refractive index  $n_e$ ) while that of the p-polarized light is perpendicular to the optic axis and converts to the ordinary mode (with refractive index  $n_o$ ). Thus,  $R_{sp} = R_{ps} = 0$  (Lekner 1994) and the exact expressions for  $R_{pp}$  and  $R_{ss}$  can be seen in supplementary materials.

Since the ellipsometric signal mainly provide the information of the p-polarized light, we can focus on  $R_{pp}$  to analyze the film information under the situation. According to eq. (S2),  $R_{pp}$  is mainly influenced by the ordinary refractive index of the film  $n_o$ . Thus, when the optic axis is normal to the plane of incidence, the ellipsometric signal is sensitive

to the ordinary refractive index of the uniaxial compressed film.

On the other hand, for the optic axis parallel to the x-direction, the s-polarization is perpendicular to the optic axis and converts completely to the ordinary mode, which gives  $R_{sp} = R_{ps} = 0$ . The exact expression for the exact expressions for  $R_{pp}$  and  $R_{ss}$  can be seen in supplementary materials. According to eq. (S10),  $R_{pp}$  is not only influenced by the extraordinary refractive index of the film  $n_e$  but the cosine of the ordinary refractive angle  $\cos\phi_o$ , or the ordinary refractive index of the film  $n_o$  since

$$\cos \phi_o = \sqrt{1 - \frac{n_1^2}{n_o^2} \sin^2 \phi_1} \tag{3}$$

However, for the film under the uniaxial stress, the ordinary refractive index  $n_o$  and the extraordinary refractive index  $n_e$  are not independent, or  $n_o$  can be interpreted as a function of  $n_e$  (detailed discussion can be seen in "Results and Analysis"). Thus, when the optic axis parallel to the x-direction, the ellipsometric signal can be used to measure the extraordinary refractive index of the uniaxial compressed film.

### Experiment Details

The experimental system is constructed by a set of ellipsometer and a stress-loading device as shown in Fig. 1. The ellipsometer based on the conventional polarizer-compensator-sample-analyzer (PCSA) configuration is used to obtain the optical variation of the sample film (Aspnes 2014). A 633 nm laser emitted by the light source falls through a polarizer P and a rotating compensator C vertically. Then the laser is reflected by the sample and vertically passes

analyzer A which is used to demodulate the polarization state of the reflection, the intensity of the light is measured by the photodetector. The single wavelength ellipsometry we used in this paper has a high sensitivity with  $\delta\psi = 0.01^\circ$ .

A gold-coating reflection mirror, a 29 mm × 17 mm SF10 glass slide with the thickness 1.5 mm is used as the sample, at the top of which a 48 nm gold film is coated for this experiment. In order to avoid the stress concentration around the boundary, the probe light is reflected by the central area of the gold coating.

In order to establish the corresponding relationship between the ellipsometry signal and the stress of the sample, a manual stress-loading device is introduced in this paper. The three-dimensional structural design drawing and physical image of the stress-loading device as shown in Fig. 1(b). The device is composed of a spring mechanism, a sample slot and an aluminum alloy pressure plate. By adjusting the nut on the outside of the spring, the six parallel springs in the spring mechanism are deformed. At this time, the pressure plate close to the sample groove will generate compression  $\sigma$  on the sample. The magnitude of the compression is determined by the displacement of the nut and the stiffness coefficient of the spring. In this experiment, the stiffness coefficient of the spring is calibrated as 274 N/m, and the displacement  $\Delta x$  of the nut can be obtained through the scales on both sides of the spring mechanism. Since the thickness of the glass substrate is much larger than that of the coating (the thickness ratio of the glass to the gold film is of the order of  $10^4$ ), the compression is mainly loaded into the glass substrate. With the deformation of the substrate, the strains at its top face would get transferred to the coated gold film which is the cause for stress in the film. At the same time, the gold coating is under the stress which changes the ellipsometric signal. The relationship between the ellipsometry signal at two orthogonal directions and the stress can be acquired by rotating the sample stage around the normal of the sample surface by  $90^\circ$ .

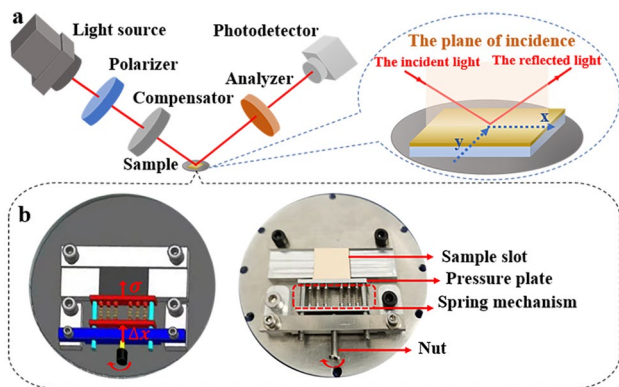


**Fig. 1** The structure schematic diagram of stress measurement using a PCSA ellipsometry: (a) the ellipsometer based on the conventional configuration and the schematic diagram of optical axes at different locations; (b) the stress-loading device

### Results and Analysis

Prior to the measurement, it is vital to adjust the measurement settings for the sample in order to improve the sensitivity of the measurement. In a common case, a sensitive measurement signal can be achieved by choosing an incident angle close to the pseudo-Brewster angle position. In Fig. 2, the ellipsometric parameter variation in which the optic axis of the sample is normal to the plane of incidence vs. angle of incidence is illustrated before and after a 35 kPa stress is applied in different colors. It can be seen that the pseudo-Brewster angle of the sample is achieved close to the incident angle of  $74^\circ$ , which is the typical pseudo-Brewster

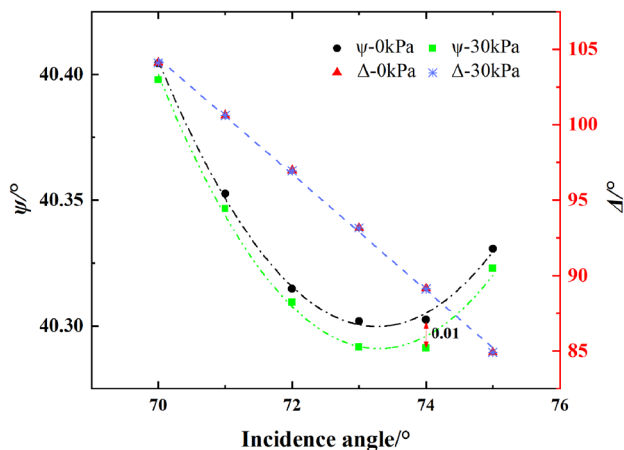


**Fig. 2** The ellipsometric parameter variation with the angle of incidence is illustrated before and after a 35 kPa stress is applied

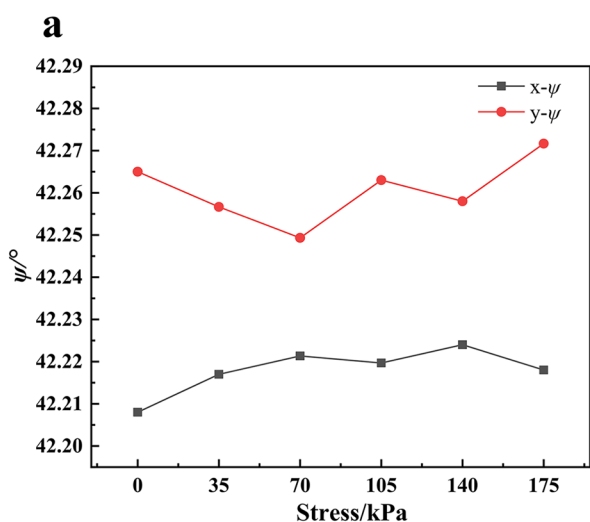
angle for gold. The maximum value of amplitude variation is about  $0.01^\circ$  achieved at this angle as the dots marked in the figure. Thus, the following stress measurements are performed at the incidence angle  $74^\circ$ .

Although the SF10 glass substrate under the uniaxial stress should exhibit anisotropic optical properties. However, the refractive index variation under the stress is negligible (see supplementary materials). Thus, we take the substrate as an isotropic support and the uniaxial optical properties mainly comes from the gold coating. As an absorbing film, the dielectric functions of the coating mainly influence the ellipsometry amplitude  $\psi$  while the phase  $\Delta$  is influenced not only by the coating but the substrate (Yang and Abelson 1995). Thus, we focus on the ellipsometry amplitude  $\psi$  to

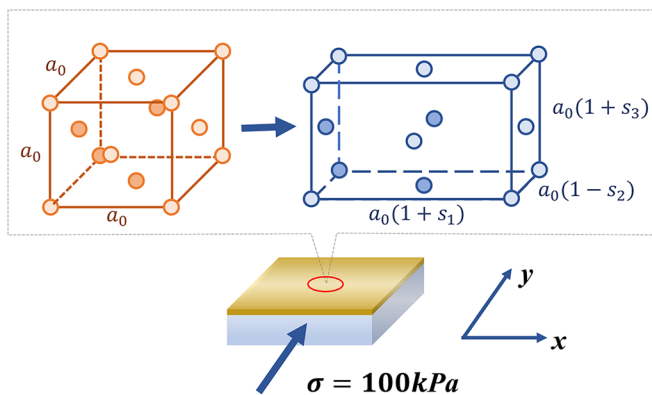
analyze the dielectric functions variation of the gold coating under the uniaxial stress.

Figure 3(a) shows the changes of the ellipsometry amplitude  $\psi$  with the stress along two orthogonal directions, x-direction and y-direction. It can be seen that trends of the amplitude parameter  $\psi$  can be divided into two parts for both directions: under the stress range of 0~70 kPa, the parameter has a linear change trend, and when the stress increases from 70 to 175 kPa, the parameter fluctuates. Since the sensitivity of  $\psi$  is around  $0.01^\circ$ , the stress sensitivity is around 35 kPa. As the first trial, we use the ellipsometry to measure the signal variation under a uniaxial stress condition. We would further to improve the sensitivity of the ellipsometry and thus more force steps would be applied to the sample. The trends of the amplitude parameter  $\psi$  indicate the deformation of the coating from the strain of the substrate. Thus, the linear change suggests the elastic deformation of the glass substrate while the fluctuation implies the yield process of the glass. A second characteristic is the opposite change trend for the two directions. Before the stress is applied, the coating is isotropic while under the uniaxial compressive stress condition, the coating shows the anisotropic uniaxial optical characteristic and we can use the ellipsometric amplitudes  $\psi_{xy}$  at the two orthogonal directions as a strain/stress indicator.

In general, the ellipsometry parameter is sensitive to the thickness and the dielectric functions of the coating film. By our estimation, the thickness variation of the film can be ignored under 100 kPa stress (see the supplementary materials). Thus, the dielectric functions variation of the coating plays a key role in the  $\psi$ -strain relationship. We



**b**



**Fig. 3** (a) The ellipsometric amplitude variation under the compression stress from 0 to 175 kPa; (b) the preliminary microscopic model of lattices change in the central region in different directions under the compression strain

could use Drude model to unveil the physics behind the  $\psi$ -strain relationship,

The dielectric functions of the metal film  $\epsilon(\omega)$  can be described by the Drude model by

$$\epsilon(\omega) = 1 - \frac{\omega_p^2}{\omega(\omega + i\gamma)} \tag{4}$$

in which  $\omega_p^2 = Ne^2/\epsilon_0 m_{eff}$ ,  $\omega_p$  is the Drude plasma frequency,  $e$ , the electric charge,  $N$  the electron density,  $m_{eff}$  the effective mass, and  $\gamma$  and the collision frequency, which is related to electron scattering processes (Ben and Park 2013).

The free electron density  $N$  for FCC metals such as gold is given by  $N = 4/a_0^3$ , where  $a_0$  is the bulk lattice constant for gold. Thus, the Drude plasmon frequency  $\omega_p$  for gold is given by

$$\omega_p^2(\omega) = \frac{4e^2}{\epsilon_0 m_{eff} a_0^3} \tag{5}$$

In general,  $\omega_p^2$  should be replaced by a second-rank tensor, Drude tensor  $\mathbf{D}$  (Mendoza and Mochán 2021) and thus, the dielectric functions of the metal are also a second-rank tensor. It can be seen from Eq. (5), a strain will induce a lattice constant variation, which will disturb the electron density  $N$ , and further the Drude plasma frequency or the Drude tensor  $\mathbf{D}$ .

For example, for an uniaxial compressive strain  $s$  where the stretching of the two other orthogonal directions can be negligible (Ben and Park 2013), an increase in the lattice constant decreases the free electron density  $N$ , and thus the plasmon frequency  $\omega_p$  for FCC metals such as gold by

$$\omega_p^2(\omega, s) = \frac{4e^2}{\epsilon_0 m_{eff} a_0^3 (1 + s)} \tag{6}$$

where  $a_0$  is the bulk lattice constant for gold.

When the stretching of the two other orthogonal directions comes into the picture, the original FCC unit cell shrinking along the  $y$  direction  $a_y = (1 + s)a_0$  while stretching along the other two directions  $a_x = a_z = a_{\parallel} = a_0 (1 + s)^{1/2}$ . Thus, an FCC lattice is converted into a BCT lattice and the Drude tensor  $\mathbf{D}$  would be appropriate to estimate the dielectric function tensor in which  $\omega_{p\parallel}^2 = \mathbf{D}_{\parallel}$  and  $\omega_{p\perp}^2 = \mathbf{D}_{\perp}$ . The detailed discussion has been studied (Mendoza and Mochán 2021).

For the ordinary refractive index  $n_o = \sqrt{\epsilon_{\parallel}}$ , where the lattice constant stretching along the electric field of the ordinary light and the extraordinary refractive index  $n_e = \sqrt{\epsilon_{\perp}}$  where the lattice constant shrinking along the electric field of the extraordinary light, the opposite strain conditions along  $x, y$  directions indicates the opposite change trends of ellipsometry amplitude  $y_x$  and  $y_y$  in Fig. 3(b) since  $y_x$  indicates the variation of  $n_e$  while  $y_x$

implies the variation of  $n_o$  as is discussed in "Ellipsometry for a Uniaxial Compressed Film".

## Conclusions

Aiming to provide a noncontact residual stress measurement method for the precision optical coating devices such as the telescopes in Taiji program, as the first trial, we use ellipsometry to detect the uniaxial stress of a gold coating reflection mirrors. Under the pseudo-Brewster angle of the gold, the stress sensitivity for the ellipsometry amplitude  $\psi$  reaches 35 kPa. The results suggest the ellipsometry response along two orthogonal directions comes from the strain-induced dielectric function tensor variations. Our preliminary microscopic model implies that the strain-induced lattice constant variation will disturb Drude tensor and the ordinary refractive index and the extraordinary refractive index under the uniaxial stress. The ellipsometry response measures the ordinary refractive index  $n_o$  when the applied force is normal to the plane incidence and measures the extraordinary refractive index  $n_e$  when the force in the plane of incidence. Thus, the ellipsometry can be used as an alternative method for the residual stress detection for the high precision optical devices with metal coatings. Further, combined with the imaging ellipsometry technique, the stress distribution can be obtained.

**Supplementary Information** The online version contains supplementary material available at <https://doi.org/10.1007/s12217-022-10017-w>.

**Acknowledgements** This work was supported by the National Key Research and Development Program of China (2020YFC2201300 and 2021YFC2202902), the Open Fund of State Key Laboratory of Applied Optics (SKLAO2020001A01), National Natural Science Foundation of China (81872584). The authors gratefully acknowledge the funding.

**Data Availability** The data that support the findings of this study are available from the corresponding author upon reasonable request.

## Declarations

**Conflict of Interest** The authors declare that they have no conflict of interest.

## References

- Abbott B.P., Abbott R., Abbott T.D., Abernathy M.R., Acernese F., Ackley K., Adams C., Adams T. et al: Observation of Gravitational Waves from a Binary Black Hole Merger. *Phys. Rev. Lett.* **116**(6), (2016a)
- Abbott B.P., Abbott R., Abbott T.D., Abernathy M.R., Acernese F., Ackley K., Adams C., Adams T. et al: GW151226: Observation



- of Gravitational Waves from a 22-Solar-Mass Binary Black Hole Coalescence. *Phys. Rev. Lett.* **116**(24), (2016b)
- Abbott B.P., Abbott R., Abbott T.D., Acernese F., Ackley K., Adams C., Adams T., Addesso P. et al: GW170817: Observation of Gravitational Waves from a Binary Neutron Star Inspiral. *Phys. Rev. Lett.* **119**(16), (2017)
- Aspnes, D.E.: Spectroscopic ellipsometry - Past, present, and future. *Thin Solid Films* **571**, 334–344 (2014)
- Azzam, R.M.A., Bashara, N.M.: Ellipsometry and Polarized Light. *Nature* **269**, 270 (1977)
- Ben X., Park H.S.: Strain engineering enhancement of surface plasmon polariton propagation lengths for gold nanowires. *Appl. Phys. Lett.* **102**(4), (2013)
- Brown, D.A., Vahi, K., Taufer, M., Welch, V., Deelman, E.: Reproducing GW150914: The First Observation of Gravitational Waves From a Binary Black Hole Merger. *Comput. Sci. Eng.* **23**(2), 73–82 (2021)
- Dubert, D., Marín-Genescà, M., Simón, M.J., Gavaldà, J., Ruiz, X.: Complementary Techniques for the Accelerometric Environment Characterization of Thermodiffusion Experiments on the ISS. *Microgravity Sci. Tec.* **31**(5), 673–683 (2019)
- Groth, B.P., Langan, S.M., Haber, R.A., Mann, A.B.: Relating residual stresses to machining and finishing in silicon carbide. *Ceram. Int.* **42**(1), 799–807 (2016)
- Gu, G., Song, B.K., Fang, M.S., Hong, Y.L., Chen, X.G., Jiang, H., Ren, W.C., Liu, S.Y.: Layer-dependent dielectric and optical properties of centimeter-scale 2D WSe<sub>2</sub>: evolution from a single layer to few layers. *Nanoscale* **11**(47), 22762–22771 (2019)
- Guo E.H., Liu Y.G., Han Y.S., Arola D., Zhang D.S.: Full-field stress determination in photoelasticity with phase shifting technique. *Meas. Sci. Technol.* **29**(4), (2018)
- Hu, W.R., Wu, Y.L.: The Taiji Program in Space for gravitational wave physics and the nature of gravity. *Natl. Sci. Rev.* **4**(5), 685–686 (2017)
- Janssen, G.C.A.M., Abdalla, M.M., van Keulen, F., Pujada, B.R., van Venrooy, B.: Celebrating the 100th anniversary of the Stoney equation for film stress: Developments from polycrystalline steel strips to single crystal silicon wafers. *Thin Solid Films* **517**(6), 1858–1867 (2009)
- Jin, G., Niu, Y.: Protein microarray biosensor based on total internal reflection imaging ellipsometry. *Febs J* **284**, 375–375 (2017)
- Labat, S., Gergaud, P., Thomas, O., Gilles, B., Marty, A.: Interdependence of elastic strain and segregation in metallic multilayers: An x-ray diffraction study of (111) Au/Ni multilayers. *J. Appl. Phys.* **87**(3), 1172–1181 (2000)
- Lekner, J.: Optical properties of a uniaxial layer. *Pure Appl. Opt.* **3**, 821–837 (1994)
- Li, Z.P., Zhang, F.H., Zhang, Y., Luo, X.C.: Experimental investigation on the surface and subsurface damages characteristics and formation mechanisms in ultra-precision grinding of SiC. *Int. J. Adv. Manuf. Tech.* **92**(5–8), 2677–2688 (2017)
- Liu, H., Luo, Z., Jin, G.: The Development of Phasemeter for Taiji Space Gravitational Wave Detection. *Microgravity Sci. Tec.* **30**(6), 775–781 (2018)
- Luo Z.R., Guo Z.K., Jin G., Wu Y.L., Hu W.R.: A brief analysis to Taiji: Science and technology. *Results Phys.* **16**, (2020)
- Luo Z.R., Wang Y., Wu Y.L., Hu W.R., Jin G.: The Taiji program: A concise overview. *Prog. Theor. Exp. Phys.* **2021**(5), (2021)
- Mendoza B.S., Mochán W.L.: Ab initio theory of the Drude plasma frequency. *J. Opt. Soc. Am. B* **38**(6), (2021)
- Nakashima S., Mitani T., Ninomiya M., Matsumoto K.: Raman investigation of strain in Si/SiGe heterostructures: Precise determination of the strain-shift coefficient of Si bands. *J. Appl. Phys.* **99**(5), (2006)
- Niu, Y., Jin, G.: Screening breast cancer by joint detection of tumor marker carbohydrate antigen 15–3 and carbohydrate antigen 72–4 with biosensor based on imaging ellipsometry. *Febs J* **284**, 268–268 (2017)
- Pflitsch, C., Muhsin, A., Bergmann, U., Atakan, B.: Growth of thin aluminium oxide films on stainless steel by MOCVD at ambient pressure and by using a hot-wall CVD-setup. *Surf. Coat. Tech.* **201**(1–2), 73–81 (2006)
- Pureza, J.M., Lacerda, M.M., De Oliveira, A.L., Fragalli, J.F., Zanon, R.A.S.: Enhancing accuracy to Stoney equation. *Appl. Surf. Sci.* **255**(12), 6426–6428 (2009)
- Ramesh, K., Ramakrishnan, V.: Digital photoelasticity of glass: A comprehensive review. *Opt. Laser. Eng.* **87**, 59–74 (2016)
- Roos, P.A., Stephens, M., Wieman, C.E.: Laser vibrometer based on optical-feedback-induced frequency modulation of a single-mode laser diode. *Appl Optics* **35**(34), 6754–6761 (1996)
- Shen J., Zhao Y., Liu H., Niu Y., Gao R., Guo T., Zhao D., Luo Z.: Multi-channel Thermal Deformation Interference Measurement of the Telescope Supporting Frame in Spaceborne Gravitational Wave Detection. *Microgravity Sci. Tec.* **34**(4), (2022)
- Sun, Y.S., Zhu, X.D.: An Ellipsometry-Based Biosensor for Label-Free, Real-Time, and in-Situ Detection of DNA-DNA and DNA-Protein Interactions. *Chinese J. Phys.* **52**(4), 1398–1406 (2014)
- van der Sneppen, L., Wiskerke, A., Ariese, F., Gooijer, C., Ubachs, W.: Improving the sensitivity of HPLC absorption detection by cavity ring-down spectroscopy in a liquid-only cavity. *Anal. Chim. Acta.* **558**(1–2), 2–6 (2006)
- Xiao, S.L., Li, B.C., Cui, H., Wang, J.: Sensitive measurement of stress birefringence of fused silica substrates with cavity ring-down technique. *Opt. Lett.* **43**(4), 843–846 (2018)
- Yang, Y.H., Abelson, J.R.: Spectroscopic ellipsometry of thin films on transparent substrates: A formalism for data interpretation. *J. Vac. Sci. Technol. A* **13**(3), 1145–1149 (1995)
- Zhang, Y., Wang, W.H., Greer, A.L.: Making metallic glasses plastic by control of residual stress. *Nat. Mater.* **5**(11), 857–860 (2006)

**Publisher's Note** Springer Nature remains neutral with regard to jurisdictional claims in published maps and institutional affiliations.

Springer Nature or its licensor holds exclusive rights to this article under a publishing agreement with the author(s) or other rightsholder(s); author self-archiving of the accepted manuscript version of this article is solely governed by the terms of such publishing agreement and applicable law.